Discrete Shearlet Transform : New Multiscale Directional Image Representation

Wang-Q Lim

Discrete Shearlet Transform : New Multiscale Directional Image Representation

Wang-Q Lim

Department of Mathematics, University of Osnabrück, Osnabrück, Germany
wlim@mathematik.uni-osnabrueck.de

Abstract:

It is now widely acknowledged that analyzing the intrinsic geometrical features of an underlying image is essentially needed in image processing. In order to achieve this, several directional image representation schemes have been proposed. In this report, we develop the discrete shearlet transform (DST) which provides efficient multiscale directional representation. We also show that the implementation of the transform is built in the discrete framework based on a multiresolution analysis. We further assess the performance of the DST in image denoising and approximation applications. In image approximation, our adaptive approximation scheme using the DST significantly outperforms the wavelet transform (up to 3.0dB) and other competing transforms. Also, in image denoising, the DST compares favorably with other existing methods in the literature.

1. Introduction

Sharp image transitions or singularities such as edges are expensive to represent and intergrating the geometric regularity in the image representation is a key challenge to improve state of the art applications to image compression and denoising. To exploit the anisotropic regularity of a surface along edges, the basis must include elongated functions that are nearly parallel to the edges.

Several image representations have been proposed to capture geometric image regularity. They include curvelets [1], contourlets [2] and bandelets [3]. In particular, the construction of curvelets is not built directly in the discrete domain and they do not provide a multiresolution representation of the geometry. In consequence, the implementation and the mathematical analysis are more involved and less efficient. Contourlets are bases constructed with elongated basis functions using a combination of a multiscale and a directional filter bank. However, contourlets have less clear directional features than curvelets, which leads to artifacts in denoising and compression. Bandelets are bases adapted to the function that is represented. Asymptotically, the resulting bandelets are regular functions with compact support, which is not the case for contourlets. However, in order to find bases adapted to an image, the bandelet transform searches for the optimal geometry. For an image of N pixels, the complexity of this best bandelet basis algorithm is $O(N^{3/2})$ which requires extensive computation [3].

Recently, a new representation scheme has been introduced [4]. These so called *shearlets* are frame elements which yield (nearly) optimally sparse representations [5]. This new representation system is based on a simple and rigorous mathematical framework which not only provides a more flexible theoretical tool for the geometric representation of multidimensional data, but is also more natural for implementations. As a result, the shearlet approach can be associated to a multiresolution analysis [4]. However constructions proposed in [4] do not provide compactly supported shearlets and this property is essentially needed especially in image processing applications. In fact, in order to capture local singularities in images efficiently, basis functions need to be well localized in the spatial domain.

In this report, we construct compactly supported shearlets and show that there is a multiresolution analysis associated with this construction. Based on this, we develop the fast discrete shearlet transform (DST) which provides efficient directional representations.

2. Shearlets

A family of vectors $\{\varphi_n\}_{n\in\Gamma}$ constitutes a *frame* for a Hilbert space $\mathcal{H}$ if there exist two positive constants A, B such that for each $f \in \mathcal{H}$ we have

$$A\|f\|^2 \leq \sum_{n\in\Gamma} |\langle f, \varphi_n\rangle|^2 \leq B\|f\|^2.$$

In the event that $A = B$, the frame is said to be *tight*.

Let us next introduce some notations that we will use throughout this paper. For $f \in L^2(\mathbb{R}^d)$, the Fourier transform of f is defined by

$$\hat{f}(\omega) = \int_{\mathbb{R}^d} f(x)e^{-2\pi i x\cdot\omega}dx.$$

Also, for $t \in \mathbb{R}^d$ and $A \in GL_d(\mathbb{R})$, we define the following unitary operators:

$$T_t(f)(x) = f(x-t)$$

and

$$D_A(f)(x) = |A|^{-\frac{1}{2}} f(A^{-1}x).$$

Finally, for $q \in (\frac{1}{2}, 1]$ and $a > 1$, we define

$$A_0 = \begin{pmatrix} a^q & 0 \\ 0 & a^{\frac{1}{2}} \end{pmatrix} \text{ and } B_0 = \begin{pmatrix} 1 & 1 \\ 0 & 1 \end{pmatrix} \qquad (1)$$

and

$$A_1 = \begin{pmatrix} a^{\frac{1}{2}} & 0 \\ 0 & a^q \end{pmatrix} \text{ and } B_1 = \begin{pmatrix} 1 & 0 \\ 1 & 1 \end{pmatrix}. \quad (2)$$

We are now ready to define a shearlet frame as follows. For $c \in \mathbb{R}^+$, $\psi_0^1, \dots, \psi_0^L, \psi_1^1, \dots, \psi_1^L \in L^2(\mathbb{R}^2)$ and $\phi \in L^2(\mathbb{R}^2)$, we define

$$\Psi_c^0 = \{\psi_{jkm}^{i,0} : j, k \in \mathbb{Z}, m \in \mathbb{Z}^2, i = 1, \dots, L\},$$

$$\Psi_c^1 = \{\psi_{jkm}^{i,1} : j, k \in \mathbb{Z}, m \in \mathbb{Z}^2, i = 1, \dots, L\},$$

and

$$\Psi_c^2 = \{T_{cm}\phi : m \in \mathbb{Z}^2\}$$

$$\cup \{\psi_{jkm}^{i,0} : j \geq 0, -2^j \leq k \leq 2^j, m \in \mathbb{Z}^2, i = 1, \dots, L\}$$

$$\cup \{\psi_{jkm}^{i,1} : j \geq 0, -2^j \leq k \leq 2^j, m \in \mathbb{Z}^2, i = 1, \dots, L\}$$

where

$$\psi_{jkm}^{i,\ell} = D_{A_\ell^{-j} B_\ell^{-k}} T_{cm} \psi_\ell^i \quad (3)$$

for $\ell = 0, 1$, $m \in \mathbb{Z}^2$, $i = 1, \dots, L$ and $j, k \in \mathbb{Z}$. If Ψ_c^p is a frame for $L^2(\mathbb{R}^2)$, then we call the functions $\psi_{jkm}^{i,\ell}$ in the system Ψ_c^p *shearlets*.

Observe that each element $\psi_{jkm}^{i,\ell}$ in Ψ_c^p is obtained by applying an anisotropic scaling matrix A_ℓ and a shear matrix B_ℓ to fixed generating functions ψ_ℓ^i. This implies that the system Ψ_c^p can provide window functions which can be elongated along arbitrary directions. Therefore, the geometrical structures of singularities in images can be efficiently represented and analyzed using those window functions. In fact, it was shown that 2-dimensional piecewise smooth functions with C^2-singularities can be approximated with nearly optimal approximation rate using shearlets. We refer to [5] for details. Furthermore, one can show that shearlets can completely analyze the singular structures of piecewise smooth images [6]. In fact, this property of shearlets is useful especially in signal and image processing, since singularities and irregular structures carry essential information in a signal. For example, discontinuities in the intensity of an image indicate the presence of edges. Figure 1 displays examples of shearlets which can be elongated along arbitrary direction in the spatial domain.

3. Construction of Shearlets

In this section, we will introduce some useful sufficient conditions to construct compactly supported shearlets. Using these conditions, we will show that the system Ψ_c^p can be generated by simple separable functions associated with a multiresolution analysis. Furthermore, this leads to the fast DST, and we will discuss this in the next section.

We first discuss sufficient conditions for the existence of compactly supported shearlets. For this, let $\alpha > \max(1, (1-p)\gamma)$ and $\gamma > \max\Big(\frac{\alpha+1}{p}, \frac{1}{1-p}\Big)$ be fixed positive numbers for $0 < p < 1$. We choose $\alpha', \gamma' > 0$ such that $\alpha' \geq \alpha + \gamma$ and $\gamma' \geq \alpha' - \alpha + \gamma$. Then we obtain the following results [7].

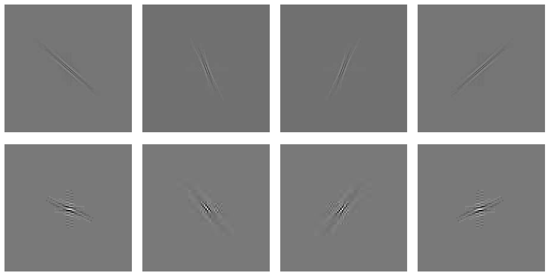

Figure 1: Examples of shearlets in the spatial domain. The top row illustrates shearlet functions $\psi_{jk0}^{i,0}$ associated with matrices A_0 and B_0 in (1). The bottom row shows shearlet functions $\psi_{jk0}^{i,1}$ associated with matrices A_1 and B_1 in (2)..

Theorem 3..1. *[7] For $i = 1, \dots, L$, we define $\psi_0^i(x_1, x_2) = \gamma^i(x_1)\theta(x_2)$ such that*

$$|\hat{\gamma}^i(\omega_1)| \leq K_1 \frac{|\omega_1|^{\alpha'}}{(1 + |\omega_1|^2)^{\gamma'/2}}$$

and

$$|\hat{\theta}(\omega_1)| \leq K_2 (1 + |\omega_1|^2)^{-\gamma'/2}.$$

If

$$\text{ess} \inf_{|\omega_1| \leq 1/2} |\hat{\theta}(\omega_1)|^2 \geq K_3 > 0 \quad (4)$$

and

$$\text{ess} \inf_{a^{-q} \leq |\omega_1| \leq 1} \sum_{i=1}^{L} |\hat{\gamma}^i(\omega_1)|^2 \geq K_4 > 0, \quad (5)$$

then there exists $c_0 > 0$ such that Ψ_c^0 is a frame for $L^2(\mathbb{R}^2)$ for all $c \leq c_0$.

Observe that the functions $\psi_0^1, \dots, \psi_0^L$ are separable functions, and the one-dimensional scaling function θ and wavelets γ^i can be chosen with sufficient vanishing moments in this case.

We now show some concrete examples of compactly supported shearlets using Theorem 3.1. Assume that $a = 4$ and $q = 1$ in (1) and (2). Let us consider a box spline [1] of order m defined as follows.

$$\hat{\theta}_m(\omega_1) = \Big(\frac{\sin \pi\omega_1}{\pi\omega_1}\Big)^{m+1} e^{-i\epsilon\omega_1},$$

where $\epsilon = 1$ if m is even, and $\epsilon = 0$ if m is odd. Obviously, we have the following two scaling equation:

$$\hat{\theta}_m(2\omega_1) = m_0(\omega_1)\hat{\theta}_m(\omega_1)$$

and

$$m_0(\omega_1) = (\cos \pi\omega_1)^{m+1} e^{-i\epsilon\pi\omega_1}.$$

Let α' and γ' be positive real numbers as in Theorem 3.1. We now define

$$\hat{\psi}_0^1(\omega) = (i)^\ell \sqrt{2} \Big(\sin \pi\omega_1\Big)^\ell \hat{\theta}_m(\omega_1)\hat{\theta}_m(\omega_2)$$

and

$$\hat{\psi}_0^2(\omega) = (i)^\ell \Big(\sin \frac{\pi\omega_1}{2}\Big)^\ell \hat{\theta}_m(\frac{\omega_1}{2})\hat{\theta}_m(\omega_2),$$

where $\ell \geq \alpha'$ and $m+1 \geq \gamma'$. Then, by Theorem 3.1, ψ_0^1 and ψ_0^2 generate a frame Ψ_c^0 for $c \leq c_0$ with some $c_0 > 0$. There are infinitely many possible choices for ℓ and m. For example, one can choose $\ell = 9$ and $m = 11$.
Define

$$\phi(x_1, x_2) = \theta_m(x_1)\theta_m(x_2),$$

$$\hat{\psi}_1^1(\omega) = (i)^\ell \sqrt{2}\Big(\sin \pi\omega_2\Big)^\ell \hat{\theta}_m(\omega_2)\hat{\theta}_m(\omega_1)$$

and

$$\hat{\psi}_1^2(\omega) = (i)^\ell \Big(\sin \frac{\pi\omega_2}{2}\Big)^\ell \hat{\theta}_m(\frac{\omega_2}{2})\hat{\theta}_m(\omega_1).$$

Then similar arguments show that ψ_1^1 and ψ_1^2 generate a frame Ψ_c^1 for $c \leq c_0$ with some $c_0 > 0$. Furthermore, the functions ϕ, ψ_ℓ^i for $\ell = 0, 1$ and $i = 1, 2$ generate a frame Ψ_c^2 with $c \leq c_0$ for some $c_0 > 0$.

4. Discrete Shearlet Transform

In the previous section, we constructed compactly supported shearlets generated by separable functions associated with a multiresolution analysis. In this section, we will show that this multiresolution analysis leads to the fast DST which computes $\langle f, \psi_{jkm}^{i,\ell}\rangle$. To be more specific, we let $a = 4$ and $q = 1$ in (1) and (2). For notational convenience, we let $n = (n_1, n_2), m = (m_1, m_2), d = (d_1, d_2) \in \mathbb{Z}^2$ and I_2 be a 2 by 2 identity matrix.
Let $\theta \in L^2(\mathbb{R})$ be a compactly supported function such that $\{\theta(\cdot - n_1) : n_1 \in \mathbb{Z}\}$ is an orthonormal sequence and

$$\theta(x_1) = \sum_{n_1 \in \mathbb{Z}} h(n_1)\sqrt{2}\theta(2x_1 - n_1). \tag{6}$$

Define

$$\gamma(x_1) = \sum_{n_1 \in \mathbb{Z}} g(n_1)\sqrt{2}\theta(2x_1 - n_1) \tag{7}$$

such that γ has sufficient vanishing moments and the pair of the filters h and g is a pair of conjugate mirror filters. We assume that γ and θ satisfy decay conditions (4) and (5) in Theorem 3.1. We also define

$$\phi(x_1, x_2) = \theta(x_1)\theta(x_2),$$

$$\psi_\ell^1(x_1, x_2) = \gamma(x_{\ell+1})\theta(x_{2-\ell}) \tag{8}$$

and

$$\psi_\ell^2(x_1, x_2) = 2^{-\frac{1}{2}}\gamma(\frac{x_{\ell+1}}{2})\theta(x_{2-\ell}) \tag{9}$$

for $\ell = 0, 1$. Then Theorem 3.1 can be easily generalized to show that the functions $\psi_0^1, \psi_0^2, \psi_1^1, \psi_1^2$ and ϕ generate a shearlet frame Ψ_c^2 with $c < c_0$ for some $c_0 > 0$.
Let J be a positive odd integer. Based on a multiresolution analysis associated with the two-scale equation (6), we can now easily derive a fast algorithm for computing shearlet coefficients $\langle f, \psi_{jkm}^{i,\ell}\rangle$ for $\ell = 0, 1, j = 1, \ldots, \frac{J-1}{2}$, and $-2^j \leq k \leq 2^j$ as follows.
First, assume that

$$f = \sum_{n \in \mathbb{Z}^2} f_J(n) D_{2^{-J}I_2} T_n \phi \tag{10}$$

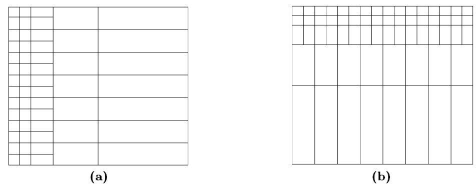

Figure 2: Examples of anisotropic discrete wavelet decomposition: (a) Anisotropic discrete wavelet decomposition by $\mathcal{W}$, (b) Anisotropic discrete wavelet decomposition by $\widetilde{\mathcal{W}}$.

where $f_J(n) = \langle f, D_{2^{-J}I_2} T_n \phi\rangle$. For $h = 0, 1$, let us define maps $\mathcal{D}_h^{k,j} : \ell^2(\mathbb{Z}^2) \to \ell^2(\mathbb{Z}^2)$ by

$$(\mathcal{D}_h^{k,j} x)(d) = \sum_{m \in \mathbb{Z}^2} d_h^{k,j}(d, m) x(m)$$

where $d_h^{k,j}(d, m) = \langle D_{B_h^{k/2^j}} T_m \phi, T_d \phi\rangle$ and $x \in \ell(\mathbb{Z}^2)$.
Also we define

$$H(\omega_1) = \sum_{n_1} h(n_1) e^{-2i\pi\omega_1}$$

and

$$G(\omega_1) = \sum_{n_1} g(n_1) e^{-2i\pi\omega_1}.$$

Finally, we let h_j, g_j^0 and g_j^1 be the Fourier coefficients of

$$\begin{cases} H_j(\omega_2) = \prod_{k=0}^{J-j-1} H\Big(2^k\omega_2\Big) \quad \text{for } J - j > 0, \\ G_j^0(\omega_1) = \prod_{k=0}^{J-2j-2} H(2^k\omega_1)G(2^{J-2j-1}\omega_1), \\ G_j^1(\omega_1) = \prod_{k=0}^{J-2j-1} H(2^k\omega_1)G(2^{J-2j}\omega_1), \end{cases} \tag{11}$$

respectively. Then we obtain

$$\begin{cases} \langle f, \psi_{jkm}^{1,0}\rangle = (((\mathcal{D}_0^{k,j} f_J) *_r \overline{h}_j)_{\downarrow 2^{J-j}} *_c \overline{g}_j^0)_{\downarrow 2^{J-2j}}(m), \\ \langle f, \psi_{jkm}^{2,0}\rangle = (((\mathcal{D}_0^{k,j} f_J) *_r \overline{h}_j)_{\downarrow 2^{J-j}} *_c \overline{g}_j^1)_{\downarrow 2^{J-2j+1}}(m), \\ \langle f, \psi_{jkm}^{1,1}\rangle = (((\mathcal{D}_1^{k,j} f_J) *_c \overline{h}_j)_{\downarrow 2^{J-j}} *_r \overline{g}_j^0)_{\downarrow 2^{J-2j}}(m), \\ \langle f, \psi_{jkm}^{2,1}\rangle = (((\mathcal{D}_1^{k,j} f_J) *_c \overline{h}_j)_{\downarrow 2^{J-j}} *_r \overline{g}_j^1)_{\downarrow 2^{J-2j+1}}(m), \end{cases} \tag{12}$$

where $*_c$ and $*_r$ are convolutions along the vertical and horizontal axes respectively, $\downarrow 2^j$ is the downsampling by 2^j and $\overline{h}(n) = h(-n)$ for given filter coefficients $h(n)$.
From (12), we observe that the shearlet transform $\langle f, \psi_{jkm}^{i,\ell}\rangle$ is the application of the shear transformation $D_{B_\ell^{k/2^j}}$ to $f \in L^2(\mathbb{R}^2)$ followed by the wavelet transform associated with anisotropic scaling matrix A_ℓ. In this case, applying $\mathcal{D}_\ell^{k,j}$ to $f_J \in \ell^2(\mathbb{Z}^2)$ corresponds to applying the shear transform $D_{B_\ell^{k/2^j}}$ in the discrete domain. Thus we simply replace the operator $\mathcal{D}_\ell^{k,j}$ by the discrete shear transform $P_{k,j}^\ell$ for $f_J \in \ell^2(\mathbb{Z}^2)$, where we define the discrete shear transforms $P_{k,j}^0$ and $P_{k,j}^1$ as follows:

$$\begin{cases} (P_{k,j}^0 f_J)(n) = f_J\big(n_1 + \lfloor (k/2^j) n_2 \rfloor, n_2\big), \\ (P_{k,j}^1 f_J)(n) = f_J\big(n_1, n_2 + \lfloor (k/2^j) n_1 \rfloor\big). \end{cases} \tag{13}$$

Let M be a fixed positive integer. Since $P_{k,j}^0$ and $P_{k,j}^1$ are unitary operators on $\ell(\mathbb{Z}^2)$, we can extend the shearlet transform defined in (12) to a linear transform S consisting of finitely many orthogonal transforms S_k^M and $\tilde{S}_k^M$ where

$$S_k^M(f_J) = \mathcal{W}P^0_{k,M}(f_J) \quad \text{and} \quad \tilde{S}_k^M(f_J) = \widetilde{\mathcal{W}}P^1_{k,M}(f_J)$$

and $\mathcal{W}$ and $\widetilde{\mathcal{W}}$ are the wavelet transform associated with an anisotropic sampling matrices A_0 and A_1, respectively. For the precise definitions of $\mathcal{W}$ and $\widetilde{\mathcal{W}}$, we refer to [7]. In this case, the linear transform S, which we call DST, is defined by

$$S = (S^M_{-2^M}, \dots, S^M_{2^M}, \tilde{S}^M_{-2^M}, \dots, \tilde{S}^M_{2^M})$$

for a given $M \in \mathbb{Z}^+$. Notice that redundancy of the DST is $K = 2^{M+2} + 2$ and the DST merely requires $O(KN)$ operations for an image of N pixels. It is obvious that the inverse DST is simply the adjoint of S with normalization.

5. Image Approximation Using DST

In this section, we present some results of the DST in image compression applications. In this case, we use adaptive image representation using the DST. The main idea of this is similar to the matching pursuit introduced by Mallat and Zhong [8]. The matching pursuit selects vectors one by one from a given basis dictionary at each iteration step. On the other hand, our approximation scheme searches the optimal directional index k_0 at each iteration step so that corresponding the orthogonal transform $S^M_{k_0}$ or $\tilde{S}^M_{k_0}$ provides an optimal nonlinear approximation with P nonzero terms among all possible $2^{M+2}+2$ orthogonal transforms in S. For a detailed description of this algorithm, we refer to [7]. For numerical tests, we compare the performance of the DST to other transforms such as the discrete biorthogonal CDF 9/7 wavelet transform (DWT)[9] and contourlet transform (CT)[2] in image compression (see Figure 3). We used only 2 directions (horizontal and vertical) and 4 level decomposition for our DST. In this case, our numerical tests indicate that only a few iterations (1-5) can give significant improvement over other transforms and computing time is comparable to the wavelet transform. For more results, we refer to [8].

6. Conclusion

We have constructed compactly supported shearlet systems which can provide efficient directional image representations. We also have developed the fast discrete implementation of shearlets called the DST. This algorithm consists of applying the shear transforms in the discrete domain followed by the anisotropic wavelet transforms.
Applications of our proposed transform in image approximation and denoising were studied. In image approximation, the results obtained with our adaptive image representation using the DST are significantly superior to those of other transforms such as the DWT and CT both visually and with respect to PSNR.
In denoising, we studied the performance of the DST coupled with a (partially) translation invariant hard tresholding estimator. Our results indicate that the DST consistently outperforms other competing transforms. For detailed numerical results, we refer to [7].

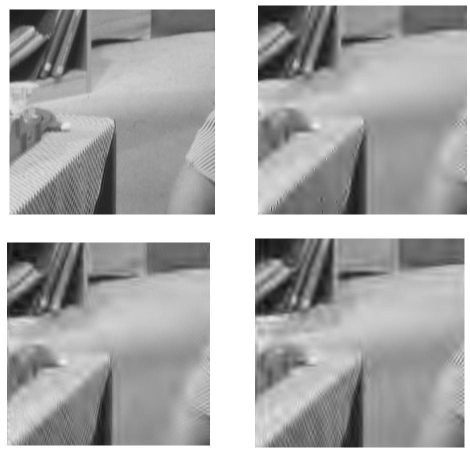

Figure 3: Compression results of 'Barbara' image of size 512×512: The image is reconstructed from 5024 most significant coefficients. **Top left:** Zoomed original image, **Top right:** Zoomed image reconstructed by the DWT (PSNR = 25.11), **Bottom left:** Zoomed image reconstructed by the CT (PSNR = 25.88), **Bottom right:** Zoomed image reconstructed by the DST with only 1 iteration step (PSNR = 26.73).

References:

[1] E. Candes and D. Donoho, "New tight frames of curvelets and optimal representations of objects with piecewise C^2 singularities," *Commun. Pure Appl. Math*, vol. 57, no. 2, pp. 219-266, Feb. 2004.

[2] M. Do and M. Vetterli, "The contourlet transform: An efficient directional multiresolution image representation," *IEEE Trans. Image Process.*, vol. 14, no. 12, pp. 2091-2106, Dec. 2005.

[3] G. Peyre and S. Mallat, "Discrete Bandelets with Geometric Orthogonal Filters," *Proceedings of ICIP,* Sept. 2005.

[4] D. Labate, W. Lim, G. Kutyniok and G. Weiss "Sparse Multidimensional Representation using Shearlets", *Proc. of SPIE conference on Wavelet Applications in Signal and Image Processing XI*, San Diego, USA, 2005.

[5] K. Guo and D. Labate, "Optimally Sparse Multidimensional Representation using Shearlets,", *SIAM J Math. Anal.*, 39 pp. 298-318, 2007.

[6] K. Guo, D. Labate and W. Lim, "Edge Analysis and identification using the Continuous Shearlet Transform", to appear in *Appl. Comput. Harmon. Anal.*

[7] W. Lim, "Compactly Supported Shearlet Frames and Their Applications", submitted.

[8] S. Mallat and S. Zhang, "Matching Pursuits With Time-Frequency Dictionaries," *IEEE Trans. Signal Process.*, pp. 3397-3415, Dec. 1993.

[9] A. Cohen, I. Daubechies and J. Feauveau, "Biorthogonal bases of compactly supported wavelets," *Commun. on Pure and Appl. Math.*, 45:485-560, 1992.